

## Performance of Ta/TaN coated titanium felt for proton exchange membrane water electrolysis

Huatao Ye<sup>a,b</sup>, Long Chen<sup>a,b</sup>, Dongchen Shen<sup>a</sup>, Song Li<sup>a,b,c,\*</sup>,  
Zhengkai Tu<sup>a,b,c,\*\*</sup>

<sup>a</sup> Department of New Energy Science and Engineering, School of Energy and Power Engineering, Huazhong University of Science and Technology, Wuhan, 430074, China

<sup>b</sup> China-EU Institute for Clean and Renewable Energy, Huazhong University of Science and Technology, Wuhan, 430074, China

<sup>c</sup> Shenzhen Research Institute of Huazhong University of Science and Technology, Shenzhen, 518057, China

### ARTICLE INFO

Handling Editor: Shohji Tsumihama

#### Keywords:

Anti-corrosion coating  
Titanium felt  
Resistance  
Water electrolysis  
Oxidization

### ABSTRACT

Metal nitride coatings, especially Ta/TaN are demonstrated to be a cost-effective anti-corrosion coating for titanium bipolar plate (BPP) of proton exchange membrane water electrolyzer (PEMWE). However, the performance of Ta/TaN coatings for titanium felt gas diffusion layer (GDL) is still elusive. In this work, Ta/TaN coated titanium felt is prepared by magnetron sputtering followed by structural characterization and electrochemical tests. It is found that its surface roughness is obviously increased after coating, while the porosity and average pore size decrease resulting from the blockage of small pore aperture on the surface upon coating. Although the anti-corrosion capability and interface contact resistance (ICR) of Ta/TaN coated titanium felt are improved, its performance in electrolytic cell assembled with Ta/TaN coated titanium felt fails in contrast to the excellent durability of PEMWE assembled with Ta/TaN coated BPP. Further scanning electron microscopy (SEM), energy dispersive X-ray spectroscopy (EDS) and X-ray photoelectron spectroscopy (XPS) confirm that Ta/TaN coatings on titanium felt in direct contact with anode catalytic layers are oxidized, resulting in remarkably increased resistance and performance failure. This study demonstrates the performance of metal nitride coating on GDL in PEMWE and inspires further efforts into the exploration of cost-effective coatings for titanium felt for PEMWE.

### 1. Introduction

In order to cope with global climate change, the world's renewable energy power generation is growing rapidly [1]. According to statistics, from 2013 to 2020, the world's renewable energy power generation increased by 45%, and it is expected to reach 40% of the total power generation by 2040 [2]. In the process of vigorously developing renewable energy in the world, due to the inherent instability and intermittent characteristics of renewable energy (such as wind energy and solar energy), it has brought great challenges to its grid-connected utilization and led to a large-scale waste of resources such as abandoning wind and light [3]. Therefore, the rapid growth of renewable energy must be matched with the corresponding energy storage system to store excess energy and make effective use of renewable energy [4]. As a secondary energy with high energy density, hydrogen energy can

effectively connect various energy networks such as gas, electricity and heat energy, promote the two-way transmission of energy, build a green, clean and efficient energy system [5,6], promote the transformation of traditional fossil energy into renewable energy, open up a new road for the upcoming energy revolution, and may redefine the technical paradigm [7–9].

The core components of proton exchange membrane electrolyzer include bipolar plate (BPP) on both anode and cathode and membrane electrode assembly (MEA) between them. MEA consists of three core parts: proton exchange membrane (PEM) in the middle, catalyst layer (CL) coated on both sides of the membrane and gas diffusion layer (GDL) on both sides of the anode and cathode. GDL, also known as porous transport layer (PTL), is a porous medium existing between bipolar plates and catalyst layers on both sides of the electrolytic cell [10]. These key components dominate the cost, performance and life of PEMWE

\* Corresponding author. Department of New Energy Science and Engineering, School of Energy and Power Engineering, Huazhong University of Science and Technology, Wuhan, 430074, China.

\*\* Corresponding author. Department of New Energy Science and Engineering, School of Energy and Power Engineering, Huazhong University of Science and Technology, Wuhan, 430074, China.

E-mail addresses: [songli@hust.edu.cn](mailto:songli@hust.edu.cn) (S. Li), [tzklq@hust.edu.cn](mailto:tzklq@hust.edu.cn) (Z. Tu).

<https://doi.org/10.1016/j.ijhydene.2024.11.057>

Received 24 August 2024; Received in revised form 28 October 2024; Accepted 3 November 2024

Available online 11 November 2024

0360-3199/© 2024 Hydrogen Energy Publications LLC. Published by Elsevier Ltd. All rights are reserved, including those for text and data mining, AI training, and similar technologies.

hydrogen production system [11]. In the cost of PEMWE stack, the cost of PEM and catalyst accounts for 5% and 8%, respectively, while the manufacturing cost of MEA is accounting for 10% [12]. In comparison, BPP and GDL account for 51% and 17% of the cost, respectively [12]. During the operation of PEMWE, BPP and GDL are in a high voltage (above 2 V), and in acidic and oxidizing corrosive environment, which limits their materials to be mainly titanium-based materials, and also requires precious metal protective coatings such as Pt and Au [13]. In order to reduce the cost of electrolytic cell, the development of cheap BPP, GDL and anti-corrosion coating materials has won increasing attention, among which developing cheap and highly durable anti-corrosion coatings for BPP and GDL has been the key [14].

In order to meet the requirements of durability and performance of PEMWE, noble metal coatings such as Pt and Au are often used in titanium GDL. For the GDL coating, Fan et al. [15] prepared an iridium-ruthenium mixed oxide coating on the surface of titanium felt, which exhibited good chemical stability, corrosion resistance and catalytic activity. When the noble metal loading is only 2 mg/cm<sup>2</sup>, the assembled PEM electrolyzer can achieve a cell pressure of 1.841 V at 2 A/cm<sup>2</sup>, outperforming the Pt-coated titanium felt. Huang et al. [16] prepared IrO<sub>2</sub>/Ti oxygen evolution anode on the surface of titanium mesh by pyrolysis method, and compared the oxygen evolution anode of single-layer and double-layer titanium mesh. It was found that the electrochemical impedance of double-layer titanium mesh decreased from 7.38 mΩ × cm<sup>2</sup> to 3.03 mΩ × cm<sup>2</sup>, and the performance of electrolytic cell was obviously improved. Liu et al. [17] deposited an Ir coating of 20–150 nm on the surface of titanium PTL by magnetron sputtering. The Ir coating on titanium fiber reduced the interfacial contact resistance between PTL and catalytic layer by 60 mΩ × cm<sup>2</sup>, and the cell pressure decreased by 81 mV at 2 A/cm<sup>2</sup>, which was ascribed to the fact that the Ir coating could inhibit the formation of TiO<sub>2</sub>. Rakousky et al. [18] conducted coating stability test on PEM electrolyzers assembled with Pt-plated PTL. They found that when the current density was too high (3 A/cm<sup>2</sup>), the ohmic resistance and mass transfer resistance of the cell increased, which was related to the partial shedding of PTL surface coating. However, at the current density of 2 A/cm<sup>2</sup>, the performance of the electrolyzer remains stable.

The high cost of noble metal coatings such as Pt and Au adds up to the cost of PEM electrolyzer. In order to develop anti-corrosion coatings with both low cost and satisfactory performance for PEM electrolyzer, metal nitride coatings were developed and tested. Previous study [19] demonstrates Ta/TaN coating with low cost showed good corrosion resistance and conductivity on the surface of titanium bipolar plate. However, the performance of Ta/TaN coating on the GDL i.e., titanium felt for PEMWE is still elusive. In this work, Ta/TaN coating on titanium GDL was prepared and their internal microstructure and surface properties were characterized. The electrochemical corrosion resistance and interface contact resistance(ICR) were also tested. In order to evaluate its electrolysis performance and durability, the tests of proton exchange membrane electrolyzer assembled with Ta/TaN coated titanium felt were also conducted and analyzed.

## 2. Methodology

### 2.1. Preparation of the GDL coatings

The 0.6 mm thick titanium felt commonly used in electrolyzers and 15 mm × 15 mm in size was selected as the sample for follow-up study. Firstly, the titanium felt was put into the prepared 0.5 M H<sub>2</sub>SO<sub>4</sub> solution for pickling to remove surface oxides, and the soaking time was 20 min. Subsequently, the titanium felt was taken out and ultrasonically cleaned using deionized water and anhydrous ethanol, respectively, for 10 min to remove impurities and attached acid. After cleaning the titanium felt, put it in an oven for 1 h, and seal it after drying. Ta/TaN coating was prepared on the surface of titanium felt by magnetron sputtering, and the preparation conditions are shown in Table 1.

**Table 1**

Deposition condition of the multilayer coatings process.

Parameters	Ta/TaN coating
Substrate temperature (°C)	200
Distance target-substrate (mm)	110
Power (W)	100
Vacuum pressure before coating (Pa)	$9.9 \times 10^{-4}$
Working pressure (Pa)	0.9
Gas	Ar/Ar:N <sub>2</sub>
Gas flow (scm)	200/195:5
Deposition time (min)	90

### 2.2. Surface characterization

In this study, the micro-morphology of Ta/TaN coating on the surface and cross section of titanium-based gas diffusion layer was observed by Scanning Electron Microscope (SEM) using Nova Nano SEM 450 field emission scanning electron microscope produced by FEI company in the Netherlands, with accelerating voltage of 50–30000 V and standard magnification of 40–400,000 times.

Laser Scanning Confocal Microscopy (LSCM) is used to observe the three-dimensional morphology of the coating surface and obtain its surface roughness data to explore the influence of the coating on its surface roughness. Three-dimensional laser microscopic imaging system adopts VK-150K made by Keys, Japan, with a total magnification of 200 times. In order to eliminate the measurement errors, three typical morphology areas are chosen for scanning of each sample to obtain the averaged roughness.

Mercury intrusion porosimetry (MIP) of AutoPore IV 9510 from American Mike Instruments was used to measure the internal porosity and pore size distribution of titanium GDL, and the influence of deposited coating on the porosity of titanium felt was explored. In order to identify the surface composition of Ta/TaN coatings after electrolysis test, X-ray photoelectron spectroscopy (XPS) was conducted on Thermo ESCALAB 250XI. The acquired XPS spectra were calibrated and the peaks were characterized.

### 2.3. Electrochemical tests

The electrochemical test adopts a typical three-electrode system, including working electrode, reference electrode and counter electrode. The working electrode is the electrode where the specimen is located. After the Ta/TaN coating was sputtered on both sides of the titanium felt, the whole titanium felt was immersed in the electrolyte with a platinum electrode clip. The reference electrode is used to determine the potential of the working electrode, which is the benchmark for measuring the potential of the working electrode. The commonly used reference electrode is Ag/AgCl electrode, and its potential is 0.207 V relative to the standard hydrogen electrode (SHE) at room temperature. The function of the counter electrode is to conduct current and form a circuit with the working electrode, and a platinum sheet of 1 cm × 1 cm was used as the counter electrode. The electrolyte is a mixed solution of 0.5 mol/L H<sub>2</sub>SO<sub>4</sub> and 2 PPM NaF, to simulate the environment of acidity and micro fluoride ion generated by PEM degradation during PEMWE operation, and the test temperature is 70 °C.

Electrochemical test methods include Open Circuit Voltage(OCP), potentiodynamic polarization test and potentiostatic polarization test. In order to keep the surface of the sample in a stable state, the sample was first immersed in electrolyte for 1 h for OCP test, and then scanned by action potential, with a scanning rate of 1 mV/s and a scanning range of 1–2 V. In order to simulate the working environment of PEMWE, an overvoltage of 2 V was applied to the sample, and the constant potential test was carried out for 4 h, and the current change was recorded. The electrochemical workstation is CHI660E produced by Shanghai Chenhua, with a potential range of ±10 V and a current range of ±250 mA.

## 2.4. ICR measurement

The electric conductivity of the coated and uncoated Ti substrate was studied by interfacial contact resistance (ICR) measurement. The ICR between the BPP and GDL was assessed using a previously reported method [20]. First, the total resistance  $R_1$  between two copper plates and the titanium felt was measured, and then the titanium sheet was placed between two titanium felts, and the total resistance  $R_2$  between the copper plates and them was measured. Finally, the interface contact resistance is calculated according to the following formula:

$$R_1 = 2R_{Cu} + 2R_{Cu/G} + R_G \quad (1)$$

$$R_2 = 2R_{Cu} + 2R_{Cu/G} + 2R_G + 2R_{G/Ti} + R_{Ti} \quad (2)$$

$$R_{G/Ti} = 1/2 (R_2 - R_1 - R_{Ti} - R_G) \quad (3)$$

In the above formula,  $R_{Cu}$  is the resistance of copper plate,  $R_{Cu/G}$  is the interface contact resistance between copper plate and titanium felt,  $R_G$  is the resistance of titanium felt,  $R_{Ti}$  is the resistance of titanium sheet, and  $R_{G/Ti}$  is the interface contact resistance between titanium sheet and titanium felt. Due to the small thickness of titanium sheet and titanium felt, its own resistance can be ignored compared with the interface contact resistance. Therefore, by measuring  $R_1$  and  $R_2$ , the ICR  $R_{G/Ti}$  between the sample and GDL can be calculated. The ICR under different pressures can be obtained by applying different pressures on both sides of the copper plate with pressure testing machine. In order to reduce the measurement error in the experiment, each group of experiments was repeated independently three times.

## 2.5. Electrolyzer tests

A PEM electrolyzer cell consisting of single-channel flow field titanium BPP was manufactured with an active surface area of  $5\text{cm} \times 5\text{cm}$ . The coating was deposited on titanium felt as GDL by magnetron sputtering under the same deposition condition as described in Section 2.1. A commercially available membrane electrode assembly (MEA) was utilized, which consists of a Nafion 117 membrane, Ir-based anode catalyst and Pt-based cathode catalyst, and the catalyst loading was  $2\text{mg}/\text{cm}^2$  and  $1\text{mg}/\text{cm}^2$ , respectively.

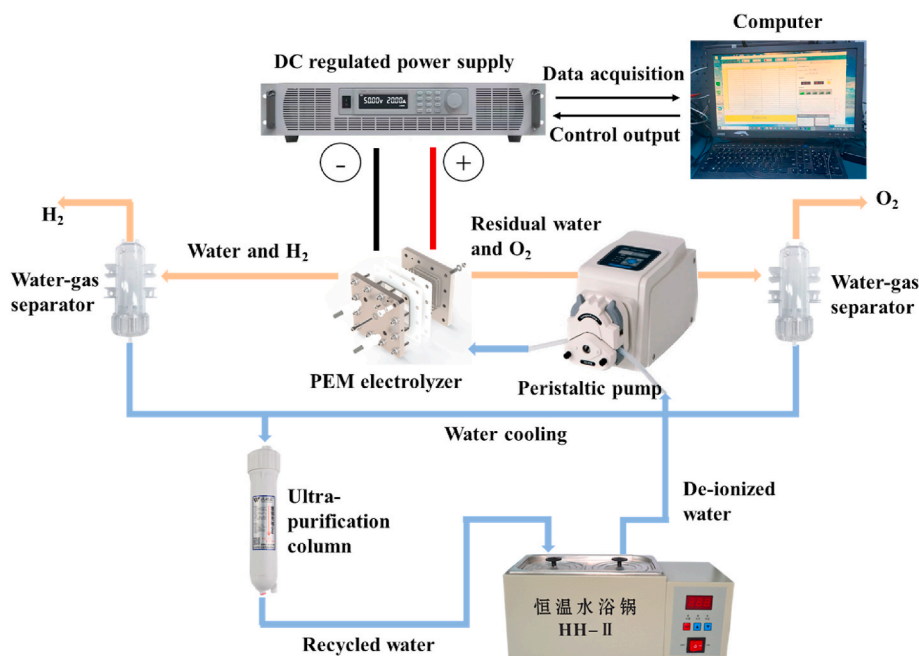
The test system of PEM electrolyzer consists of a programmable high-power DC power supply, computer, constant-temperature water bath, peristaltic pump, water-gas separator, ultra-purification column, PEM electrolyzer and heating plate. The test system is shown in Schematic 1. In addition, a 24 V DC power supply is used to supply power to the heater. Ultrapure water with the resistivity of  $18\text{M}\Omega \times \text{cm}$  was used, which was heated to  $80^\circ\text{C}$  and supplied to the anode side by a peristaltic pump at a flow rate of  $40\text{ml}/\text{min}$ . MEA was first activated prior to tests by increasing the voltage from  $1.4\text{V}$  to  $2.0\text{V}$  at  $0.1\text{V}/15\text{min}$  and then operated at a constant voltage for  $24\text{h}$  until the current density stopped rising. All tests of electrolyzers were carried out after activation.

## 3. Results and discussion

### 3.1. Characterization

According to SEM images of titanium felt before and after coating with Ta/TaN (Fig. 1), there is no obvious difference observed at low magnification (Fig. 1a and b), and titanium fibers with smooth surfaces are intricately distributed on the surface. At high magnification (Fig. 1c), the surface roughness of titanium fiber was inspected. With increasing magnification, the Ta/TaN coating grains on the surface of titanium fiber can be clearly observed (Fig. 1d). Although titanium fiber possesses uneven surface, the Ta/TaN coating is still evenly covered on its surface, and distributed at the cracks and protrusions of the substrate with uniform grain size distribution. Such a result demonstrates that the Ta/TaN coating prepared by magnetron sputtering can be well combined with uneven surface of titanium fiber substrate of GDL.

Further element distribution was obtained by scanning the titanium felt in Fig. 1e with energy dispersive X-ray spectrometer (EDS). It is found that the distribution of Ta and N elements of the coatings tends to be consistent (Fig. 1f and h), while the distribution area of the Ti element is staggered from that of the Ta element (Fig. 1g), corresponding to the areas beneath the surface of fibers that are not effectively covered by the coatings. Such results manifest that the Ta/TaN coating is mainly deposited on the titanium fibers on the surface of the titanium felt during magnetron sputtering, and no coatings in the internal porous regions were observed due to the obstruction of the titanium fibers. The quantitative surface element content analysis of Ta/TaN coated titanium



Schematic 1. Schematic diagram of the test system for proton exchange membrane electrolyzer.

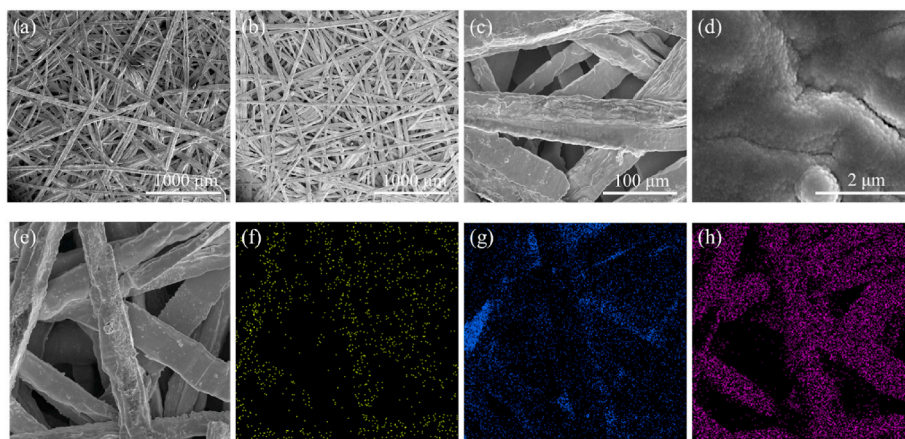


**Fig. 1.** (a) and (b) respectively show uncoated and Ta/TaN coated titanium felt; (c) and (d) are SEM images of Ta/TaN coated titanium felt at different magnifications, respectively. (e) image of titanium felt and its (f)N element (g)Ti element (h)Ta element from EDS.

felt (Table 2) demonstrates that the atomic percentage of Ta element and N element is about 3:5, probably corresponding to  $Ta_3N_5$ . The atomic percentage of the Ti element corresponding to the uncoated surface is 11.58%, which is small.

The surface roughness of uncoated titanium felt and Ta/TaN coated titanium felt was further analyzed according to the 3D scanning images of Fig. 2, and the parameters describing surface roughness were provided in Table 3.  $S_a$  is the arithmetic average height, which is often used to represent the average roughness of the surface.  $S_z$  is the maximum height of the surface.  $S_{dr}$  is the interface expansion area ratio, which refers to the ratio of the actual surface area of the defined area to the two-dimensional planar area. After coating Ta/TaN, the surface roughness  $S_a$  of titanium felt increased obviously, from 17.73  $\mu\text{m}$  to 22.38  $\mu\text{m}$ , and the maximum height  $S_z$  of the surface increased from 231.20  $\mu\text{m}$  to 276.49  $\mu\text{m}$ . It is worth noting that after coating, the interfacial expansion area ratio  $S_{dr}$  of titanium felt increased significantly, from 2.56 to 4.18, implicating that the actual surface area of coated titanium felt is significantly enlarged upon coating, which may favor the electrolysis efficiency owing to the increased interfacial area between catalytic layer and GDL.

### 3.2. Porosity and pore size analysis of titanium felt

The porous structure of titanium felt plays an important role in the gas transportation performance of GDL, thus the porosity and pore size of Ta/TaN coated titanium felt were further analyzed. The porosity and pore size distribution of titanium felt with and without coating were analyzed by processing the SEM images (Fig. 3a and b) using the professional image software ImageJ. Using the threshold adjustment function of ImageJ software, the images shown in Fig. 3c and d can be obtained, in which black areas represent titanium fibers and white areas represent pores. The pore size distribution can be obtained by calculating the pixel area of each white area, and the surface porosity of titanium felt is expressed by the percentage of white area.

According to Table 4, the surface porosity of uncoated titanium felt is 48.58%, which is slightly higher than titanium felt coated with Ta/TaN coating (43.28%). In contrast, the average pore size of uncoated titanium felt is 19.45  $\mu\text{m}$ , which is significantly lower than coated titanium

felt with an average pore size of 31.07  $\mu\text{m}$ . Such a result demonstrates the possibility that the small pore aperture or pits on the titanium felt surface may be filled by coated Ta/TaN during magnetron sputtering, thus reducing the percentage of small pores and the decreased porosity. In contrast, the average pore diameters were increased owing to the elimination of small pores.

We further measure the internal porosity of titanium felt by the mercury intrusion method. The pore structure parameters of titanium felt from the mercury intrusion method are presented in Table 5. It is found that after coating, the porosity of titanium felt decreased from the initial 66.29%–65.91%, which was consistent with the trend of surface porosity above. The most probable pore size representing the dominant pore size in SI is 58.73  $\mu\text{m}$  for the uncoated sample and 58.77  $\mu\text{m}$  for coated one, respectively, indicating that Ta/TaN coating imposes an insignificant impact on the most probable pore diameters. The average pore diameter increases from 47.26  $\mu\text{m}$  to 50.30  $\mu\text{m}$ , which is consistent with the trend from image analysis, but their pore sizes are much larger than the average pore size obtained by image analysis. The increased average pore size of coated titanium felt proves again that the Ta/TaN coating may block some small-sized pores on the surface, resulting in a decreased number of small pores and a slightly decreased porosity.

### 3.3. Corrosion resistance analysis

The electrochemical corrosion capability of coated titanium felt was tested. Open circuit potentials (OCP) is the voltage difference between the working electrode and the reference electrode under open circuit, which is one of the key parameters to evaluate the anti-corrosion capability of coatings under zero current. The higher the OCP, the higher anti-corrosion capability of the coatings under zero current. It can be found that the OCP of both uncoated and Ta/TaN coated titanium felt decreases rapidly at first and then tends to be stable in Fig. 4a. The OCP of Ta/TaN coated titanium felt is obviously higher than uncoated one, and their stable OCP values are  $-0.24\text{ V}$  and  $-0.69\text{ V}$ , respectively, indicating the increased anti-corrosion performance upon coating. However, compared with the OCP of coated titanium sheet (0.054 V) [19], the OCP of Ta/TaN coated titanium felt is obviously lower, which can be ascribed to the fact that the majority of titanium fibers in the titanium felt are not coated with Ta/TaN, and the exposed titanium fibers inside reduce the OCP of the sample compared with planar titanium.

The potentiodynamic polarization curves of uncoated and Ta/TaN coated titanium felt at  $-1\sim 2\text{ V}$  (vs  $\text{ag}/\text{AgCl}$ ) potential were presented in Fig. 4b. The corrosion voltage, corrosion current density, anode Tafel slope and cathode Tafel slope can be obtained by extrapolation of Tafel curve in the range of equilibrium potential  $\pm 60\text{ mV}$  (Table 6). It can be

**Table 2**

Contents of elements on the surface of titanium felt coated by Ta/TaN Coating.

Element	Weight percentage(%)	Atomic percentage(%)
Ta	81.47	31.50
N	10.59	56.92
Ti	7.94	11.58

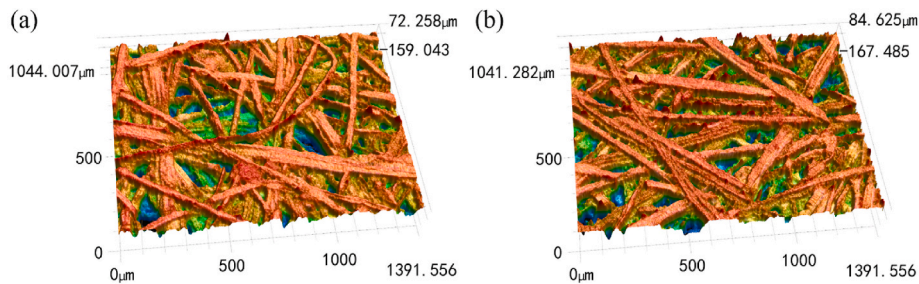


Fig. 2. 3D images of (a) uncoated titanium felt and (b) Ta/TaN coated titanium felt.

**Table 3**  
Surface roughness of uncoated titanium felt and Ta/TaN coated titanium felt.

element	Sa(μm)	Sz(μm)	Sdr
Uncoated titanium felt	17.73	231.20	2.56
Ta/TaN coated titanium felt	22.38	276.49	4.18

seen that compared with uncoated titanium felt, the corrosion voltage of Ta/TaN coated titanium felt increased from  $-0.66$  V to  $-0.56$  V, and the trend of corrosion decreased. The corrosion current density decreased from  $3.13$  mA/cm<sup>2</sup> to  $2.22$  mA/cm<sup>2</sup>, and the corrosion reaction rate decreased obviously. Such results demonstrate that the corrosion resistance of titanium felt is improved upon coating with Ta/TaN on its surface.

Compared with the corrosion current density ( $9.1$  μA/cm<sup>2</sup>) of Ta/TaN coated titanium sheet in the previous work [18], the corrosion current density of titanium felt is increased by about 1~3 orders of magnitude, which may be mainly affected by the increased surface area of the titanium felt exposed to the electrolyte. According to the interfacial expansion area ratio  $Sdr = 4.18$  of coated titanium felt in Table 3, the surface area of coated titanium felt is 4.18 times of the titanium sheet

substrate of identical size in theory. Thus, assuming the exposed area of titanium sheet to electrolyte is  $1$  cm<sup>2</sup>, the exposed area of titanium felt to electrolyte will be  $4.18$  cm<sup>2</sup>, resulting in the enhanced corrosion current density of titanium felt than titanium sheet.

**Table 4**  
Surface porous parameters of uncoated and Ta/TaN coated titanium felt.

Sample	Surface porosity(%)	Mean pore size(μm)
Uncoated titanium felt	48.58	19.45
Ta/TaN coated titanium felt	43.28	31.07

**Table 5**  
Pore parameters of uncoated and Ta/TaN coated titanium felt from mercury intrusion method.

Sample	Porosity (%)	dominant pore size (μm)	mean pore size (μm)
Uncoated titanium felt	66.29	58.73	47.26
Ta/TaN coated titanium felt	65.91	58.77	50.30

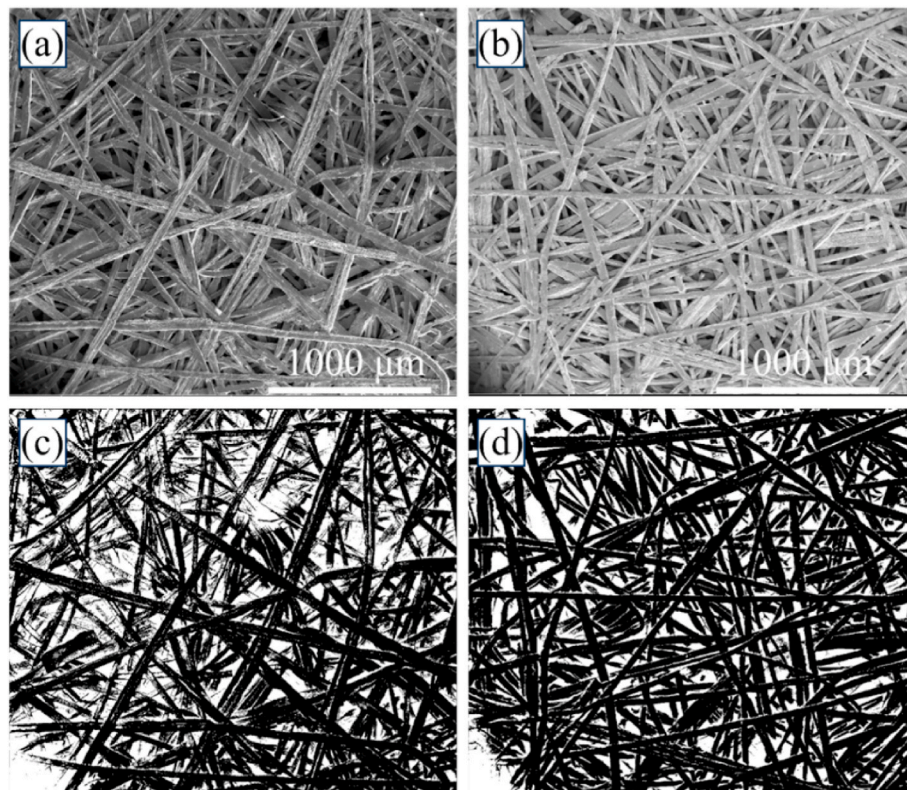
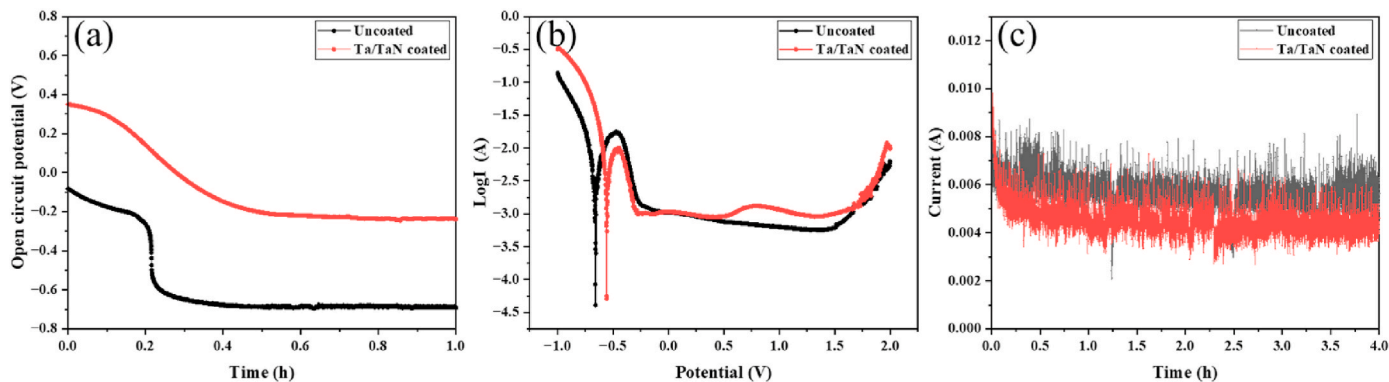


Fig. 3. Initial SEM images of the titanium felt (a) before and (b) after coating, and SEM images of the titanium felt (c) before and (d) after adjusting the threshold.



**Fig. 4.** (a) Open circuit potential-time curves of uncoated and Ta/TaN coated titanium felt; (b) Potentiodynamic scanning polarization curves of uncoated titanium felt and Ta/TaN coated titanium felt (−1~2 V vs. Ag/AgCl reference electrode); (c) Constant potential polarization curves of uncoated titanium felt and Ta/TaN coated titanium felt (2 V vs. Ag/AgCl reference electrode).

**Table 6**

Electrochemical parameters of uncoated and Ta/TaN coated titanium felt in a simulated PEMWE environment.

Sample	$E_{corr}(V)$	$I_{corr}(mA/cm^2)$	$\beta_a(mV)$	$\beta_c(mV)$	$R_p(\Omega \times cm^2)$
Uncoated titanium felt	−0.66	3.13	215.98	164.45	18.0
Ta/TaN coated titanium felt	−0.56	2.22	794.91	146.86	22.5

Fig. 4c shows the polarization curves of uncoated and Ta/TaN coated titanium felt at a constant potential of 2 V (vs ag/AgCl). The evident current fluctuation may be ascribed to porous titanium felt with a complex surface structure by comparing with the smooth polarization curves of planar titanium substrate in previous study [19]. The average current of uncoated titanium felt in a relatively stable state is 1.22 mA/cm<sup>2</sup> in potentiostatic test, while the average current density of coated titanium felt is 0.96 mA/cm<sup>2</sup>, implying that Ta/TaN coating can reduce the corrosion rate of titanium felt with a protective efficiency of 21.31%.

### 3.4. Interface contact resistance

The interface contact resistance(ICR) between titanium felt and titanium bipolar plate under varying pressures in Fig. 5 and ICR at a

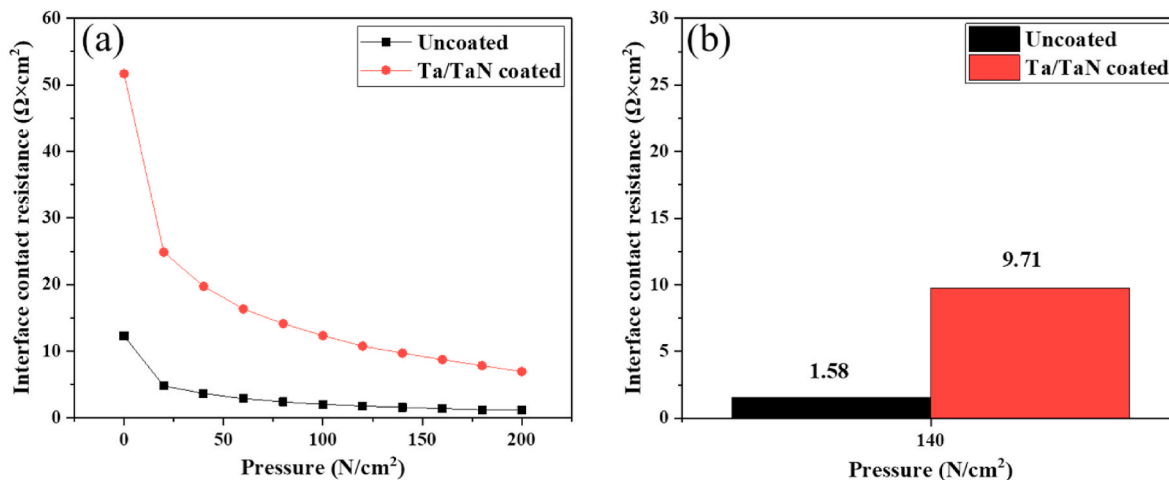


**Fig. 5.** The interface contact resistance between uncoated titanium felt and Ta/TaN coated titanium felt and titanium bipolar plate is (a) at different pressures and (b) at 140 N/cm<sup>2</sup> pressure.

pressure of 140 N/cm<sup>2</sup> in Fig. 5b demonstrates that the interfacial contact resistance between coated titanium felt and titanium bipolar plate is higher than the uncoated sample. Under the pressure of 140 N/cm<sup>2</sup> which is the commonly used pressure to assemble titanium felt into single-cell electrolyzer, the ICR between uncoated titanium felt and titanium bipolar plate is 1.58 mΩ × cm<sup>2</sup>, while the ICR increases to 9.71 mΩ × cm<sup>2</sup> after coating with Ta/TaN, which may be related to the increased surface roughness after coating. The increased surface roughness (Table 3) of coated titanium felt decreased the contact area with the titanium bipolar plates, which leads to a significant increase in interface contact resistance. Such a trend is opposite to Ta/TaN coated titanium bipolar plates [19].

### 3.5. Performance of electrolytic cell based on Ta/TaN coated titanium felt

The electrolytic performance of the cell assembled with uncoated and Ta/TaN coated titanium felt, respectively, was measured. The anode bipolar plate of the electrolytic cell is Pt coated titanium bipolar plate, and the cathode bipolar plate is an uncoated titanium bipolar plate. Fig. 6a records the current density with time in electrolyzers during the activation process. It can be found that although the current density of the electrolytic cell with Ta/TaN coated titanium felt is obviously higher than that with uncoated titanium felt at initial, its current density decreases more rapidly with time, implicating that the electrolytic cell based on Ta/TaN coated titanium felt has failed. The polarization curves of two electrolyzers after activation in Fig. 6b display the abnormally

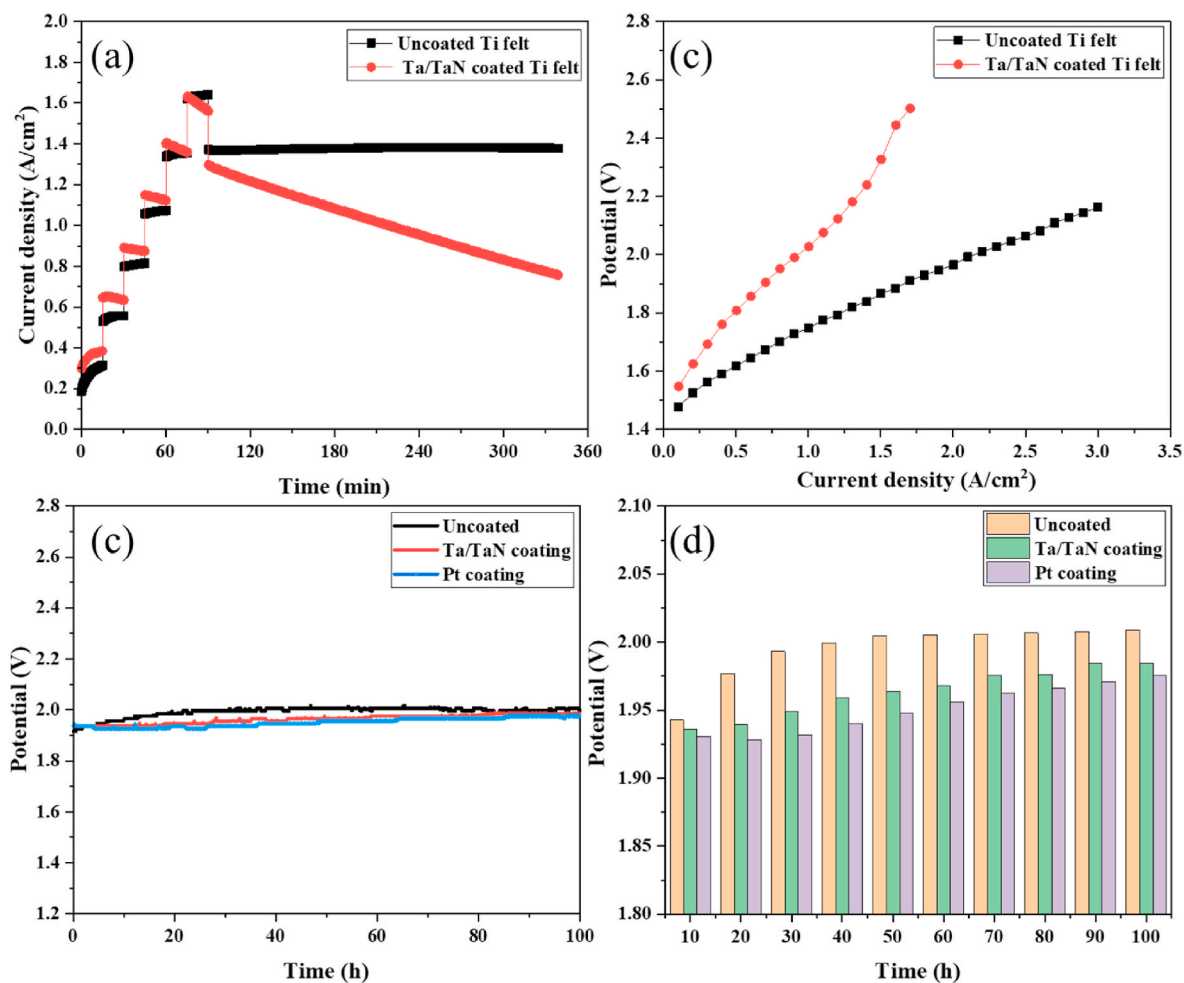


Fig. 6. (a) Current density-time curves of electrolyzers with uncoated and Ta/TaN coated titanium felt during the MEA activation process. (b) Polarization curves of electrolyzers with uncoated and Ta/TaN coated titanium felt. (c) The voltage of the electrolyzer assembled with uncoated, Ta/TaN and Pt coated anode titanium BPP during 100 h test at 2 A/cm<sup>2</sup>; (d) voltage of electrolyzers every 10 h at 2 A/cm<sup>2</sup>.

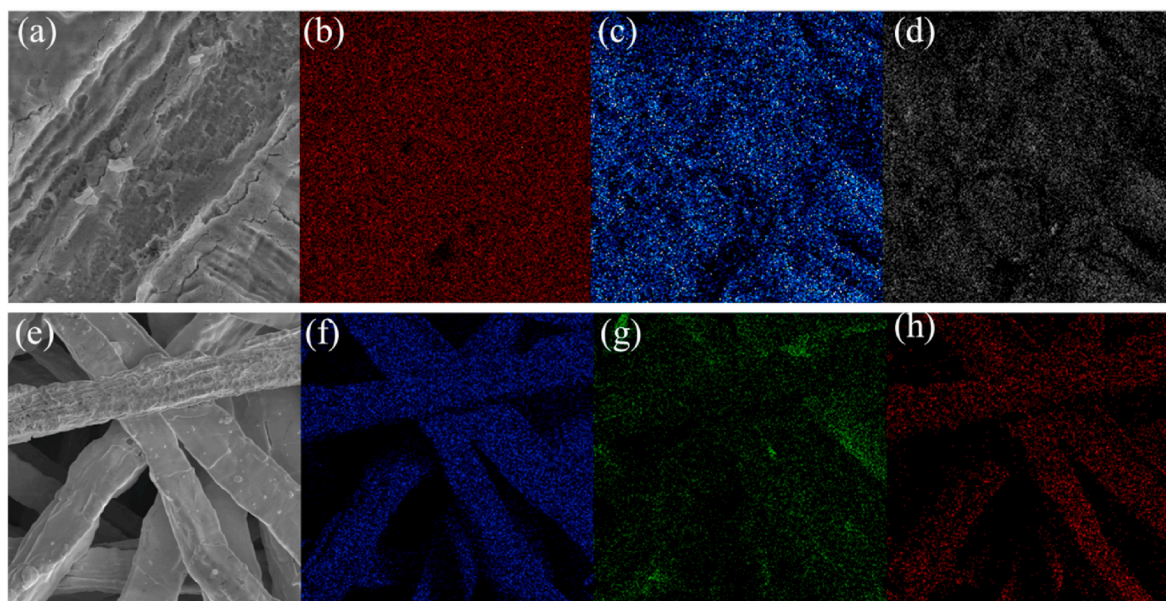


Fig. 7. (a) SEM image and corresponding element ((b) Ir, (c) O, (d) Ta) distribution of anode catalytic layer after test. (e) SEM image and element distribution ((f) Ta, (g) Ti, (h) O) of Ta/TaN coated titanium felt after electrolytic water operation.

increased voltage of the cell based on Ta/TaN coated titanium felt, suggesting the failure of the electrolytic cell with Ta/TaN coating titanium felt. Since its performance declined rapidly, it can be inferred that the Ta/TaN coating on the titanium felt may be seriously corroded and the generated oxide layer may greatly enhance the resistance of electrolyzer cell.

On the contrary, the Ta/TaN coating on titanium BPP which is not in direct contact with the anode catalytic layer exhibits high stability and durability even after a 100 h test in assembled electrolyzer as shown in Fig. 6c and d. It can be seen that the voltage of the electrolyzer assembled with uncoated titanium BPP rises rapidly, and reaches a constant voltage of 2.009 V after about 60 h with an attenuation rate of 0.662 mV/h. In comparison, the electrolytic cells with Ta/TaN and Pt coating operate stably with relatively low cell voltage, and their attenuation rates are 0.489 mV/h and 0.451 mV/h, respectively. Although the durability of Ta/TaN coating is slightly lower than Pt coating, the cost of Ta/TaN coating is low.

In order to further explore the failure mechanism of Ta/TaN coated titanium felt, the proton exchange membrane coated with catalyst and Ta/TaN coated titanium felt were further characterized. The SEM image of the anode catalytic layer after the test in Fig. 7a is gully-like, which is caused by the close contact with titanium felt and deformation under the assembly pressure when the electrolytic cell is assembled. The membrane electrode needs to be dried before the SEM test, leading to some fine cracks in its SEM image. According to the element contents of the anode catalyst layer in Table 7, it can be seen that the majority of the anode catalyst surface is Ir, followed by oxygen probably from the iridium oxide. However, a small amount of Ta element was observed with the atomic percentage of 0.78%, which may be resulted from the peeling or dissolution of Ta/TaN coating.

SEM and EDS were used to analyze the elements of the Ta/TaN coated titanium felt after operation in Fig. 7e–h. According to element contents on the surface of Ta/TaN coated titanium felt in Table 8, the fiber structure of Ta/TaN coated titanium felt did not change obviously, but there was no N element in it and the content of O element increased rapidly with the atomic percentage of 51.74%. This phenomenon may be due to the oxidation of the outermost TaN coating. In the element distribution diagram, the distribution of O element and Ta element is basically identical, which also proves this view. But the chemical reaction of Ta/TaN coating in the process of electrolytic water still needs further study.

In contrast, such a phenomenon has not been observed on the Ta/TaN coating on the titanium bipolar plate [19], indicating that the direct contact between the titanium felt and the anode catalytic layer may cause chemical reactions under oxidative environment resulting from continuously generated oxygen at anode side. To verify such an assumption and the chemical composition of coatings after the test, XPS measurement of Ta/TaN coatings on titanium felt after the electrolysis test was performed as shown in Fig. 8. The Ta 4f spectra of the coatings in Fig. 8a display two typical peaks at the binding energies of 28.3 eV and 26.3 eV, respectively, corresponding to the presences of Ta<sup>5+</sup> ions in Ta<sub>2</sub>O<sub>5</sub> [21]. The deconvoluted O1s spectra in Fig. 8b manifest three peaks at binding energies of 530.7 eV, 531.7 eV and 533.1 eV, corresponding to the presence of Ta–O [22], C=O, C–O, respectively [23]. Because of the limitation of XPS measurement, the sampling depth of XPS is usually below 10 nm. Thus, the oxidized samples cannot be exactly quantified currently. Nevertheless, XPS results confirmed the occurrence of oxidation of Ta/TaN coatings of titanium felt upon contact with an anode catalytic layer under electrolysis conditions.

**Table 7**

Element contents of anode catalyst surface after test.

Element species	Ir	O	Ta
Weight percentage(%)	76.50	21.04	2.46
Atomic percentage(%)	23.06	76.16	0.78

**Table 8**

Element contents of the surface of Ta/TaN coatings on titanium felt after test.

Element species	Ta	Ti	O	N
Weight percentage(%)	84.87	5.22	9.91	0
Atomic percentage(%)	39.16	9.10	51.74	0

In summary, regardless of the outstanding electrolysis performance of the electrolytic cell assembled with Ta/TaN coated BPP, the electrolytic cell assembled with Ta/TaN coated titanium felt fails during the activation process, which can be ascribed to the chemical oxidation of Ta/TaN coatings in contact with anode catalytic layers, leading to rapidly increased resistance resulting from the produced oxide layer on titanium surface. The generated oxide layer may further inhibit the oxygen evolution reaction of water, leading to the decreased catalytic activity of catalytic layer. Thus, Ta/TaN coating is not applicable to titanium felt according to the above tests.

#### 4. Conclusion

In this study, Ta/TaN coated titanium felt prepared by magnetron sputtering was characterized, tested and analyzed to assess its micro-structure and anti-corrosive capability in the simulated proton exchange membrane water electrolysis environment. The impacts of the surface coating on the structure and internal porosity of titanium felt were investigated by scanning electron microscope (SEM), laser scanning confocal microscope (LSCM) and mercury intrusion meter. It is found that the Ta/TaN coating on the surface of the titanium felt is evenly distributed, but there is almost no Ta/TaN coating inside the titanium felt. Compared with uncoated titanium felt, the surface roughness of Ta/TaN coating increases from 17.73  $\mu\text{m}$  to 22.38  $\mu\text{m}$ , which is one reason for the increased interface contact resistance from 1.58  $\text{m}\Omega \times \text{cm}^2$  to 9.71  $\text{m}\Omega \times \text{cm}^2$ . Besides, the surface porosity of titanium decreased from 48.58% to 43.28% after coating, and its internal porosity slightly decreased from 66.29% to 65.91%. However, the average pore diameter increased from 47.26  $\mu\text{m}$  to 50.30  $\mu\text{m}$ , resulting from the blockage of small pores owing to coating.

The corrosion resistance of Ta/TaN coating on the surface of titanium felt was studied by electrochemical test. It is revealed that Ta/TaN coating is beneficial to improve the corrosion resistance of titanium felt with the corrosion voltage increased from  $-0.66$  V to  $-0.56$  V, the corrosion current density decreased from 3.13  $\text{mA}/\text{cm}^2$  to 2.22  $\text{mA}/\text{cm}^2$ , and the polarization resistance increased from 18.0  $\Omega \times \text{cm}^2$  to 22.5  $\Omega \times \text{cm}^2$ . The protective efficiency of Ta/TaN coating on titanium felt is estimated to be 21.31%, which is lower than that of Ta/TaN coating on the titanium bipolar plate. The performance of the electrolyzer assembled with Ta/TaN coated titanium felt decreased rapidly in the operating environment during activation. Through the elemental analysis of the catalytic layer and the titanium felt, it is found that the catalytic layer contains a small amount of Ta element, and there is no N element on the surface of the titanium felt. XPS analysis confirmed that Ta/TaN coating of titanium felt in direct contact with the anode catalytic layer was oxidized, leading to rapidly increased resistance and performance failure of PEMWE. Such phenomena were not observed in our previous electrochemical test of the Ta/TaN coating on the titanium BPP and the electrolyzer assembled with Ta/TaN coated titanium BPP exhibited high stability even after the 100 h test. In future, the anti-oxidation activity of coatings on titanium felt should be also taken into consideration. This work paves the way for the applicability of metal nitride coating on GDL surface and the findings in this work may be extended to other metal nitride coatings of GDL in PEMWE. This work may also inspire further efforts into the exploration of cost-effective coatings for titanium felt in PEMWE in the future.



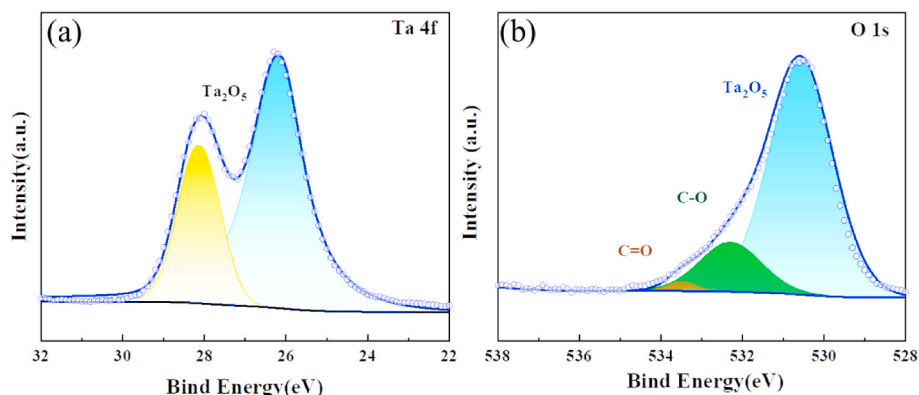


Fig. 8. XPS spectra of (a) Ta 4f and (b) O1s of Ta/TaN coated titanium felt after 100 h-electrolysis operation.

### CRediT authorship contribution statement

**Huatao Ye:** Writing – original draft, Visualization, Validation, Methodology, Investigation, Formal analysis, Data curation. **Long Chen:** Writing – original draft, Visualization, Investigation, Formal analysis, Data curation. **Dongchen Shen:** Visualization, Validation, Investigation, Formal analysis, Data curation. **Song Li:** Writing – review & editing, Supervision, Software, Resources, Project administration, Methodology, Investigation, Funding acquisition, Formal analysis, Conceptualization. **Zhengkai Tu:** Writing – review & editing, Supervision, Software, Resources, Project administration, Methodology, Investigation, Formal analysis, Conceptualization.

### Declaration of competing interest

The authors declare that they have no known competing financial interests or personal relationships that could have appeared to influence the work reported in this paper.

### References

- [1] Zhang S, Zhang X, Rui Y, Wang R, Li X. Recent advances in non-precious metal electrocatalysts for pH-universal hydrogen evolution reaction. *Green Energy Environ* 2021;6:458–78.
- [2] Parra D, Valverde L, Pino FJ, Patel MK. A review on the role, cost and value of hydrogen energy systems for deep decarbonisation. *Renew Sustain Energy Rev* 2019;101:279–94.
- [3] Wang S, Geng Z, Bi S, Wang Y, Gao Z, Jin L, et al. Recent advances and future prospects on Ni3S2-Based electrocatalysts for efficient alkaline water electrolysis. *Green Energy Environ* 2024;9:659–83.
- [4] Hou X, Yang L, Hou K, Shi H, Feng L, Suo G, et al. Hydrolysis hydrogen production mechanism of Mg10Ni10Ce alloy surface modified by SnO2 nanotubes in different aqueous systems. *Green Energy Environ* 2021;6:124–37.
- [5] Ma Z, Cheng Z, He Y. Experimental study of the steady and dynamic efficiencies of a solar methanol steam reforming reactor filled with a phase change material for hydrogen production. *J Tsinghua Univ (Sci Technol)* 2021;61:1371–8.
- [6] Zheng H, Han F, Sata N, Costa R. Hydrogen production at intermediate temperatures with proton conducting ceramic cells: electrocatalytic activity, durability and energy efficiency. *J Energy Chem* 2023;86:437–46.
- [7] Hosseini SE, Wahid MA. Hydrogen from solar energy, a clean energy carrier from a sustainable source of energy. *INT J ENERG RES* 2020;44:4110–31.
- [8] Zhao Y, Yu Z, Ge A, Liu L, Faria JL, Xu G, et al. Direct seawater splitting for hydrogen production: recent advances in materials synthesis and technological innovation. *Green Energy Environ* 2024.
- [9] Fahad Aldosari O, Hussain I, Malaibari Z. Emerging trends of electrocatalytic technologies for renewable hydrogen energy from seawater: recent advances, challenges, and techno-feasible assessment. *J Energy Chem* 2023;80:658–88.
- [10] Ito H, Maeda T, Nakano A, Hwang CM, Ishida M, Kato A, et al. Experimental study on porous current collectors of PEM electrolyzers. *INT J HYDROGEN ENERG* 2012;37:7418–28.
- [11] Wang C, Yu L, Yang F, Feng L. MoS2 nanoflowers coupled with ultrafine Ir nanoparticles for efficient acid overall water splitting reaction. *J Energy Chem* 2023;87:144–52.
- [12] Babic U, Suermann M, Büchi FN, Gubler L, Schmidt TJ. Critical review-identifying critical gaps for polymer electrolyte water electrolysis development. *J Electrochem Soc* 2017;164:F387–99.
- [13] Gago AS, Ansar SA, Saruhan B, Schulz U, Lettenmeier P, Cañas NA, et al. Protective coatings on stainless steel bipolar plates for proton exchange membrane (PEM) electrolyzers. *J Power Sources* 2016;307:815–25.
- [14] Schmidt O, Gambhir A, Staffell I, Hawkes A, Nelson J, Few S. Future cost and performance of water electrolysis: an expert elicitation study. *INT J HYDROGEN ENERG* 2017;42:30470–92.
- [15] Fan Z, Yu H, Jiang G, Chi J, Sun S. A low-cost Ti felt anode gas diffusion layer for PEM water electrolysis. *Chin J Power Sources* 2020;44:933–6.
- [16] Mina H, Gaoyanga L, Xindong W. Synthesis and performance of multilayered titanium mesh oxygen evolution anode in polymer exchange membrane water electrolysis. *Nonferrous Metals Science and Engineering* 2016;7:1–5.
- [17] Liu C, Carmo M, Bender G, Everwand A, Lickert T, Young JL, et al. Performance enhancement of PEM electrolyzers through iridium-coated titanium porous transport layers. *Electrochem Commun* 2018;97:96–9.
- [18] Rakousky C, Keeley GP, Wippermann K, Carmo M, Stolten D. The stability challenge on the pathway to high-current-density polymer electrolyte membrane water electrolyzers. *Electrochim Acta* 2018;278:324–31.
- [19] Ye H, Tu Z, Li S. Electrochemical performance of metal nitride coated titanium bipolar plate for proton exchange membrane water electrolyser. *J Power Sources* 2024;595:234052.
- [20] Wang H. Stainless steel as bipolar plate material for polymer electrolyte membrane fuel cells. *J Power Sources* 2003;115:243–51.
- [21] Xu J, Bao XK, Fu T, Lyu Y, Munroe P, Xie Z. In vitro biocompatibility of a nanocrystalline  $\beta$ -Ta2O5 coating for orthopaedic implants. *Ceram Int* 2018;44:4660–75.
- [22] Xu J, Peng S, Jiang S, Munroe P, Xie Z. Erosion–corrosion resistance of a  $\beta$ -Ta 2 O 5 nanocrystalline coating in two-phase fluid impingement environments. *MATER SCI TECH-LOND*. 2019;35:925–38.
- [23] Feng Y, Yang Q, Wang X, Logan BE. Treatment of carbon fiber brush anodes for improving power generation in air–cathode microbial fuel cells. *J Power Sources* 2010;195:1841–4.